ELSEVIER

Polymer 43 (2002) 2287–2294

polymer

www.elsevier.com/locate/polymer

Effects of NCO/OH molar ratio on structure and properties of graft-interpenetrating polymer networks from polyurethane and nitrolignin

Jin Huang, Lina Zhang*

Department of Chemistry, Wuhan University, Wuhan 430072, People's Republic of China

Received 31 July 2001; received in revised form 13 December 2001; accepted 15 December 2001

Abstract

A series of graft-interpenetrating polymer networks (graft-IPNs) with different NCO/OH molar ratio was synthesized from castor oil-based polyurethane (PU) and nitrolignin (NL) by changing the content of 1,4-butanediol as chain-extender. The effects of NCO/OH molar ratio on the morphology and properties of the PU–NL films (UL) were investigated by infrared, wide-angle X-ray diffraction (WAXD), differential scanning calorimetry, dynamic mechanical analysis, and tensile test. WAXD patterns showed that all the UL films were nearly amorphous. With an increase in NCO/OH molar ratio, the glass transition temperature (T_g), the stiffness and tensile strength (σ_b) increased, while the breaking elongation (ε_b) and strain recoverability (Re) decreased. The UL films with 1.20 of NCO/OH molar ratio exhibited the maximum value of tensile strength ($\sigma_b = 30.2$ MPa; $\varepsilon_b = 152\%$). 2.8 wt% NL plays an important role in the simultaneous enhancement of σ_b and ε_b of the UL films. Solid-state ^{13}C nuclear magnetic resonance (^{13}C NMR) showed that the introduction of NL into PU restricted the motion of PU molecules, indicating a relatively high cross-link network structure in the UL films. Therefore, a relatively great network structure like a star by grafting with multi-PU networks on a NL molecule as the graft-IPNs model was deduced in this work.

Keywords: Graft-IPNs; Nitrolignin; Polyurethane

1. Introduction

Polyurethane (PU) is a class of very useful and versatile materials to meet diverse needs. Segmented PUs are regarded as multi-block copolymers of $(AB)_n$ type, where A and B represent the hard- and soft-segment repeat units, respectively. Usually, the hard-segment provides physical cross-links through hydrogen bonding and filler-like reinforcement to the soft-segment, which plays a key role in imparting the elasticity to PU materials [1]. The compositions, concentration and NCO/OH molar ratio in the hard-segment can affect the structure, organization and flexibility of the hard-segment, and the sequent microphase separation and mechanical properties of PU [2–14]. Therefore, the NCO/OH molar ratio is regarded as an efficient way to regulate the morphology and properties of PUs. The hard-segment of PU is generally formed in a polyaddition reaction between diisocyanate and a multi-functional alcohol or amine with low molecular weight (60–400). The PUs with different NCO/OH molar ratios are usually synthesized by changing chain-extender content under constant contents of other components. It is worth noting that the allophanate chemical cross-links formed due to excess diisocyanate as NCO/OH > 1 have a detrimental effect on the hard-segment domains with physical cross-links [11]. The increase of such chemical cross-links leads to a reduction in size and numbers of hard-segment domain, and causes microphase mixing to form a more homogeneous network in segmented PU elastomers [12,13]. These kinds of morphological changes result in the shift of glass transition temperature (T_g) to a higher temperature and a broadening effect on the glass transition region with an increase of NCO/OH molar ratio [13]. Moreover, hydroxyl terminated polybutadiene (HTPB)-based PU with a higher NCO/OH molar ratio exhibits higher stress and lower strain at break mainly due to the increase of intermolecular attraction of hard to hard-segments [14].

Interpenetrating polymer networks (IPNs) are a specific type of polymer blend composed of cross-linked polymers via intermolecular permanent entanglements and interpenetrations [15]. Moreover, graft-IPNs, a IPNs system containing graft-reactions between the polymeric components, can

* Corresponding author. Tel.: +86-27-87219274; fax: +86-27-8788-2661.

E-mail address: lnzhang@public.wh.hb.cn (L. Zhang).

0032-3861/02/$ - see front matter
PII: S0032-3861(02)00028-9

enhance compatibility of the component and the microphase heterogeneity, and hence improve some properties of the constituent materials [16]. Graft-IPNs composed of PU and epoxy, exhibited higher tensile strength and thermal stability than the simple PU [17]. In our laboratory, graft-IPN material from chitosan and PU, has been satisfactorily prepared. It exhibits good mechanical properties and biodegradability [18,19]. Lignin is a nontoxic, commercially available and low-cost renewable resource that has the potential to be utilized as a basic raw material in the chemical industry [20]. In previous work [21], castor oil-based PU–nitrolignin (UL) films have been satisfactorily prepared. It is proved that nitrolignin (NL) has a high reactivity with PU to form a graft-IPNs structure, resulting in an enhancement of toughness and strength of the UL films. A basic understanding of the effect of NCO/OH molar ratio on the structure and properties is essential for successful applications of the UL materials. In this paper, the UL films with various NCO/OH molar ratios were prepared, and their structure and properties were investigated by spectroscopic methods, thermal analysis and tensile test. The relationships between morphology and properties as well as the effect of NL were further discussed.

2. Experimental

2.1. Materials

All the chemical reagents were obtained from commercial sources in China. Castor oil, chemically pure, was dehydrated at 100 °C under 20 mmHg for 1 h. Alkali lignin from bamboo was supplied by Guangzhou Chemistry Institute of China. 2,4-toluene diisocyanate (TDI) was redistilled before use. 1,4-butanediol (BDO) is of chemical purity.

2.2. Preparation of nitrolignin

NL was prepared by reacting alkali lignin with fuming nitric acid and acetic anhydride added by droplet under an ice/salt bath for 12 h with stirring. After the reaction, the solid precipitate was removed by ultracentrifuge, then washed with water until neutral, followed by drying in vacuum for seven days to obtain the powder with reddish brown color. Nitrogen content of the NL was determined to be 8.08% by Heraeus Elemental Analyzer (CHN-O-RAPID, German), and the weight-average molecular weight (M_w) to be 19.2×10^4 by a multi-angle laser light scattering (DAWN-DSP, Wyatt Technology Co. USA).

2.3. Preparation of UL

A three-necked flask was fitted with a nitrogen inlet tube, a mechanical stirrer, and a pressure-equalizing dropping funnel. Castor oil was added drop-by-drop into the flask with TDI under a nitrogen atmosphere at 45 °C. The dropping was completed in 30 min, and then the stirring was stopped after 20 min to yield PU prepolymer with a 2.0 molar ratio of NCO/OH. The equivalent weights 345 g per –OH of castor oil and 87 g per –NCO of TDI were used to calculate the added weight of castor oil and TDI.

Table 1
The compositions of UL films prepared from PU prepolymer with 0.0116 mol/0.0058 mol of NCO/OH molar ratio, BDO and 2.8 wt% NL (PU series have the corresponding compositions except for no addition of NL)

Sample	BDO–OH (mol)	NCO/OH molar ratio of PU
UL-B0	–	2.0
UL-B1	0.0006	1.8
UL-B2	0.0019	1.5
UL-B3	0.0039	1.2
UL-B4	0.0052	1.05
UL-B5	0.0078	0.85
UL-B6	0.0101	0.73

PU prepolymer/tetrahydrofuran (THF), NL/THF and BDO/THF solutions were mixed and stirred for 0.5 h at room temperature. The obtained mixture was cast on the glass plate, and then dried in the air for 1 h followed by curing at 35 ± 2 °C for 7 h. The films were removed from the glass plate and coded as UL-B0–UL-B6 with NCO/OH molar ratio from 2.0 to 0.73. NCO/OH molar ratios were regulated by the changes of BDO content, while keeping the content of NL constant at 2.8 wt%. The compositions of the UL films are listed in Table 1. The corresponding PU films were prepared by a similar process without the addition of NL, and coded as PU-B0–PU-B6.

2.4. Characterization

Fourier transform infrared spectroscopy (FTIR) spectra of the UL films were taken by using a KBr plate on a Spectrum One FTIR (Perkin–Elmer Instruments, USA) in a range of wavenumber from 4000 to 400 cm^{-1}. Solid-state ^{13}C nuclear magnetic resonance (^{13}C NMR) experiments were performed on a Bruker MSL-400 NMR spectrometer equipped with a 3.6-T superconducting magnet at 25 °C, and the spectra were obtained by cross-polarization with magic angle spinning at 5.0 kHz.

Wide-angle X-ray diffraction (WAXD) patterns of the UL films were recorded on D/max-1200 X-ray diffractometer (Rigaku Denki, Japan) with Cu Kα radiation ($\lambda = 1.5405 \times 10^{-10}$ m), and the samples were examined with 2θ ranging from 6 to 40° at a scanning rate of 5° min^{-1}.

Differential scanning calorimetry (DSC) measurement of the UL films was carried out on a DSC-2C thermal analyzer (Perkin–Elmer Co., USA). The heating rate was 10 °C min^{-1} in the temperature range of −50–240 °C. Dynamic mechanical analysis (DMA) tests of the UL films were performed on a DMA 242 dynamic mechanical analyzer (Netzsch Co., German) under an air atmosphere at a frequency of 33.3 Hz, and the temperature ranged from −100 to 150 °C with a heating rate of 10 °C min^{-1}.

Tensile strength (σ_b) and breaking elongation (ε_b) of the PU and UL films were measured on a universal testing machine (CMT6503, Shenzhen SANS Test Machine Co. Ltd, China) with a tensile rate of 100 mm min^{-1} according to ISO6239-1986 (E). Samples of UL and PU films were all marked to be 50 mm length l_0, and then snapped on a machine mentioned earlier with a tensile rate of 100 mm min^{-1}. To evaluate the recoverability of the films, the length l_1 of broken sheets was determined repeatedly after 12 h intervals. The recoverability of dimension (Re) is represented by

$$\mathrm{Re} = \frac{l_0 - \Delta l}{l_0} 100\%$$

where Δl is the length of irrecoverable creep after 12 h and equals to $l_1 - l_0$.

3. Results and discussion

3.1. Effects of NCO/OH molar ratio on structure

Fig. 1 shows IR spectra of UL-B0 and the characteristic functional groups for the UL films with the various NCO/OH molar ratios. The –NH stretching vibration bands are thought to be composed of hydrogen-bonded –NH (3350 cm^{-1}) and free –NH (3444 cm^{-1}), while –C=O bands consist of hydrogen-bonded –C=O in ordered crystalline domains (1702 cm^{-1}) and in disordered amorphous domains (1714 cm^{-1}), and free –C=O (1734 cm^{-1}) [22]. The –NH in PU is mainly hydrogen-bonded with –C=O in hard-segments and the ether- or ester-oxygen of soft-segments. When NCO/OH molar ratio was higher than 1.20, the chemical cross-links from excess –NCO restricted the formation of urethane –NH, resulting in the decrease of intensity for free –NH with an increase of NCO/OH molar ratio. When NCO/OH molar ratio was lower than 1.20, the intensity of free –NH of the UL films increased with a decrease of NCO/OH molar ratio caused by the shielding effect of excess BDO, which is verified by the increase of –OH absorption between 3200 and 3300 cm^{-1} contributing to excess BDO and unreacted NL. In addition, the changes of free –NH as shown, indicated that 1.20 of NCO/OH molar ratio for UL-B3 may be a turning point for the combined effects of the graft-reaction of NL, chemical cross-links and hydrogen-bonds. In this case, –C=O can be hydrogen-bonded with –OH of NL and BDO or the urethane –NH. The intensity of hydrogen-bonded –C=O for the UL films increased with a decrease of NCO/OH molar ratio except for UL-B6, which exhibited the strongest free –C=O vibration. With a decrease of NCO/OH molar ratio, more –OH from excess BDO and unreacted NL hydrogen-bonded with –C=O, resulting in an increase of absorption of hydrogen-bonded –C=O. It is obvious that the increase of BDO content would restrict the reaction between NL and PU networks. Thus, excess BDO in

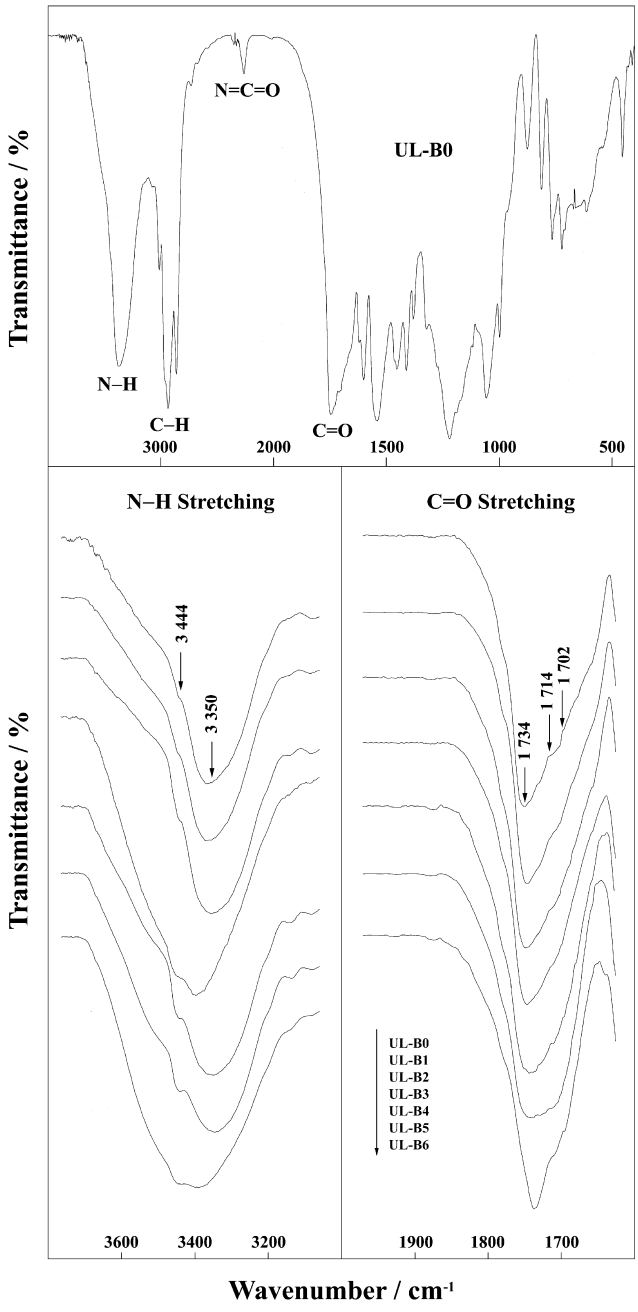

Fig. 1. FTIR spectra of UL-B0 and the characteristic functional groups of the UL films with different NCO/OH molar ratios.

UL-B6 with 0.73 of NCO/OH molar ratio changed the original structure and destroyed hydrogen-bonds, causing a sharp increase of free –C=O absorption. It suggests that the formation of PU network is prior to the reaction of NL and –NCO to form graft-IPN structure, namely higher NCO/OH molar ratio facilitated the graft-reaction between NL and PU network.

The glass transition temperature (T_g) is usually used to evaluate the mobility of soft-segment and microphase separation between hard- and soft-segment in PU. Fig. 2 shows DSC thermograms and T_g (onset) of the UL films,

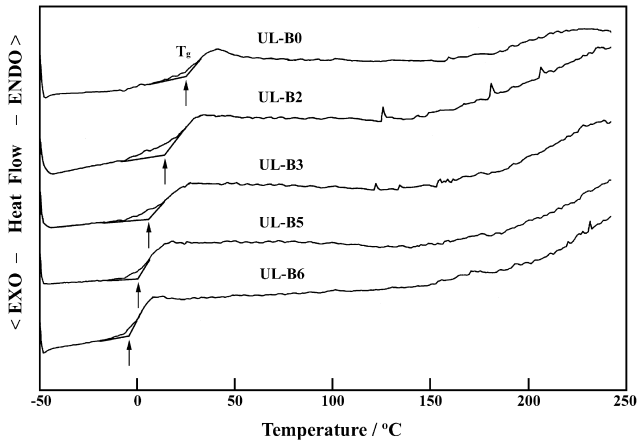

Fig. 2. DSC thermograms of the UL films with different NCO/OH molar ratios.

and the detailed information is listed in Table 2. T_g of the UL films was shifted to higher temperature with an increase of NCO/OH molar ratio, but the heat-capacity (ΔC_p) hardly changed. It can be explained that excess –NCO in UL with relatively high NCO/OH molar ratio can further react with each other to form three-dimensional allophanate or biuret cross-links, resulting in an increase of T_g. It has been reported that the shift to higher temperature of PU T_g in a grafted semi-IPNs may be caused by grafting onto the PU networks to cause some restriction of the segmental motion [23]. T_g can also reflect the influence of hard-segment structure on the mobility of the soft-segment units as indicated by the gradual broadening of the glass transition region [13]. As shown in Table 2, the T_g range for the UL films obviously broadened with an increase of NCO/OH molar ratio, and both $T_{g,b}$ and $T_{g,e}$ also increased simultaneously. This suggests that the extent of microphase mixing increased with an increase of chemical cross-links. In addition, the graft-IPN structure based on NL and PU network also restricted the motion of soft-segment, and hence enhanced $T_{g,b}$, $T_{g,e}$ and broadened glass transition range.

Fig. 3 shows the storage modulus (log E') and tan δ as a function of temperature for the UL films by DMA, and the data of T_g, T_{max}, log E' at T_g and height of loss peak are summarized in Table 3. The DMA technique generally

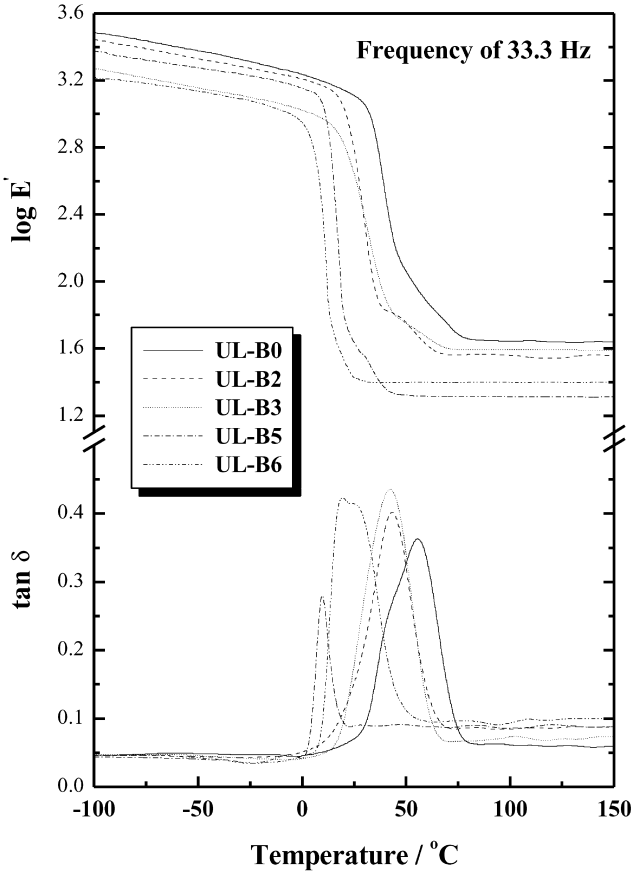

Fig. 3. Storage modulus (log E') and tan δ as functions of temperature for the UL films with different NCO/OH molar ratios.

provides higher T_g values than DSC (up to 10 °C higher), due to the dynamic nature of the test [24]. T_g and T_{max} for the UL films significantly increased with an increase of NCO/OH molar ratio similar to the changes of T_g from DSC. Moreover, the broadening effect in α transition region of loss peak caused by NCO/OH molar ratio was also in good agreement with that for the glass transition from DSC. With an increase of NCO/OH molar ratio, the values of log E' at T_g (onset) increased up to maximum value for UL-B3, and then slightly decreased, indicating that the stiffness of the film UL-B3 was higher than others. As shown in tan δ–T curves, the shape of loss peaks implied that the mobility of molecular chain in the soft-segment matrix was diverse. The peaks of UL-B0 and UL-B5 consisted of a main peak and a shoulder peak, but other UL films, especially UL-B6, exhibited a single peak. It indicated that there are two

Table 2
DSC data of the UL films with different NCO/OH molar ratios ($T_{g,b}$ and $T_{g,e}$ represent the beginning and ending temperature of the glass transition region, respectively)

Sample no.	UL-B0	UL-B2	UL-B3	UL-B5	UL-B6
T_g (onset) (°C)	23.97	13.63	5.22	0.43	− 4.09
T_g range (°C)	63.11	40.67	44.88	43.01	28.53
$T_{g,b}$ (°C)	6.85	7.63	16.98	16.98	18.85
$T_{g,e}$ (°C)	69.96	33.04	27.90	26.03	9.68
$\Delta C_{p,g}$ ($\times 10^2$ J g^{-1} K^{-1})	–	39.67	37.41	38.36	40.28

Table 3
DMA data of the UL films with different NCO/OH molar ratios

Sample no.	UL-B0	UL-B2	UL-B3	UL-B5	UL-B6
T_g (onset) (°C)	31.1	17.7	19.3	10.5	6.3
Log E' at T_g (onset)	3.00	3.13	3.16	3.14	2.97
T_{max} (°C)	55.7	43.2	42.8	19.2	9.6
Height of loss peak	0.364	0.427	0.442	0.424	0.284

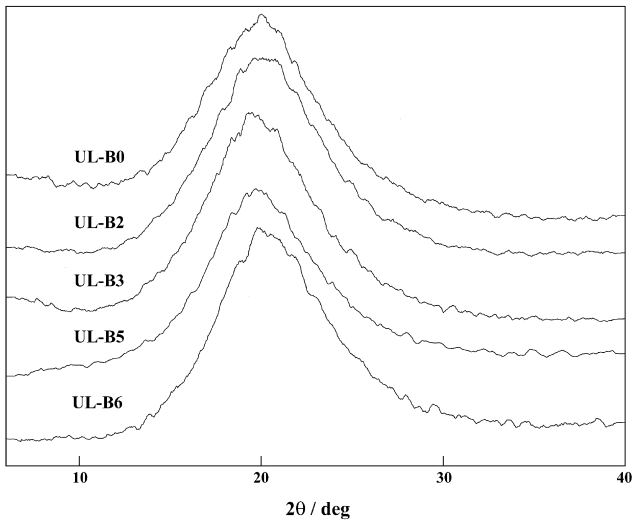

Fig. 4. WAXD patterns of the UL films with different NCO/OH molar ratios.

kinds of chain mobility for soft-segment in the α transition region for UL-B0 (chemical cross-links due to –NCO and graft-reaction due to NL) and UL-B5 (excess BDO in soft-segment matrix and graft-reaction due to NL), resulting in the enhancement of microphase separation between soft- and hard-segments [25]. The single peak of UL-B2 and UL-B3 suggested that with a decrease of NCO/OH molar ratio the chemical cross-links caused by excess –NCO decreased, and the narrow peak for UL-B6 represented that excess BDO restricted the graft-reaction between NL and PU network and the chemical cross-links.

Fig. 4 shows the WAXD patterns of the UL films with different NCO/OH molar ratio. Obviously, a broad diffraction peak for each UL film indicated the amorphous nature. This suggests that no hard-segment domain was separated from the well-mixed mixture even at high NCO/OH molar ratio. This is well consistent with observations of DSC measurement with no obvious endothermic absorption above T_g.

3.2. Effects of NCO/OH molar ratio on properties

The effects of NCO/OH molar ratio on σ_b and ε_b of UL films and the corresponding PU films are shown in Fig. 5. With an increase of NCO/OH molar ratio, ε_b values of UL films decreased, but σ_b values increased up to maximum value at 1.2 of NCO/OH molar ratio for UL-B3, resulting from the relative high chemical cross-linking that can restrict the chain mobility and increase the intermolecular attraction of hard to hard-segments [14]. Interestingly, both σ_b and ε_b of the UL films were much higher than those of the corresponding PU films, and especially σ_b and ε_b of UL-B3 with NCO/OH molar ratio 1.20 were, respectively, triple and 1.5 times than those of PU-B3. This indicated that the introduction of NL plays a key role in the improvement of mechanical properties due to the formation of graft-IPNs.

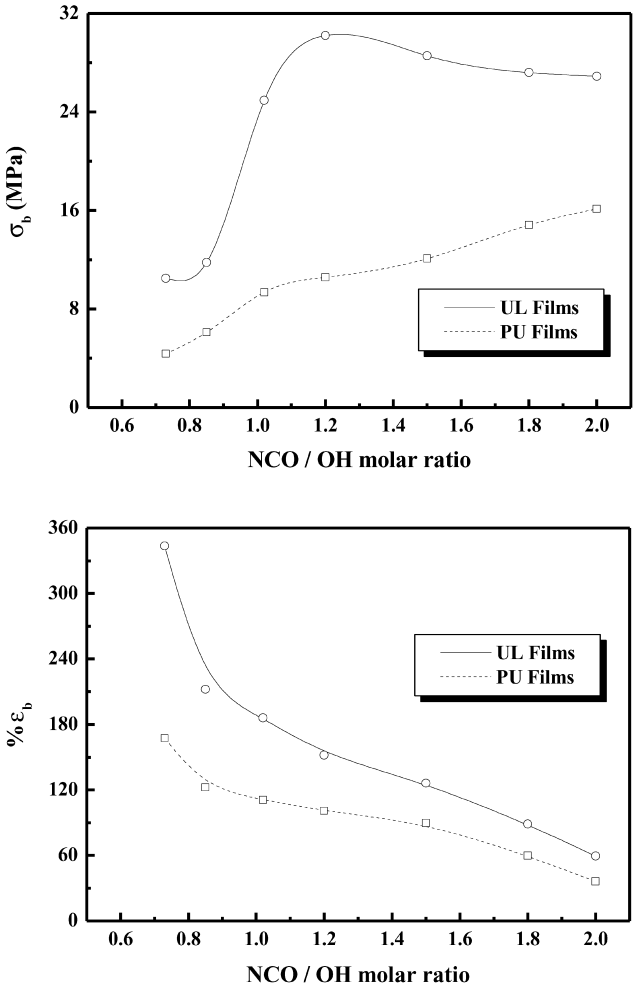

Fig. 5. Mechanical properties (σ_b and ε_b) of the UL films as a function of NCO/OH molar ratios compared with corresponding PU films.

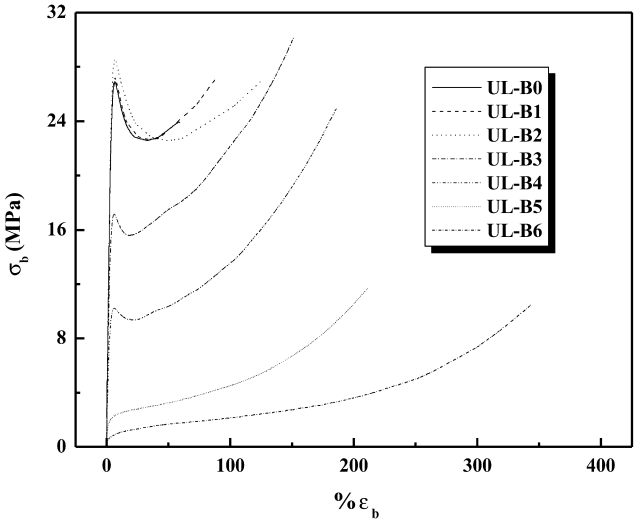

Fig. 6. Stress-strain curves of the UL films with different NCO/OH molar ratios.

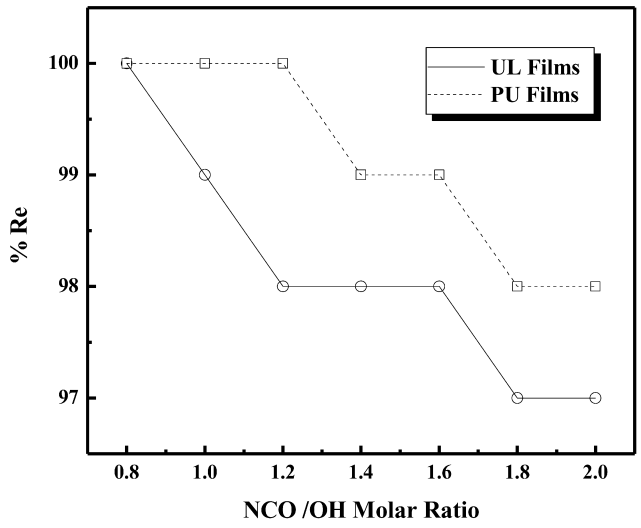

Fig. 7. Strain recoverability of the UL films as a function of NCO/OH molar ratios compared with corresponding PU films.

Fig. 6 shows the stress–strain curves of UL films with different NCO/OH molar ratio. The UL-B0–UL-B4 films exhibited a yield-point that represents the transition from rubber to plastics, and the strength at yield for ULB0-ULB2 was higher than that at break for UL-B0–UL-B2. However, the UL-B5 and UL-B6 films with lower NCO/OH molar ratio have no yield-point, suggesting a rubber-like, corresponding to the lower T_g and weaker tan δ peaks. Strain recoverability (Re) of the UL films and PU films are shown in Fig. 7. Both the UL and corresponding PU films exhibited excellent strain recoverability, which increased with a decrease of NCO/OH molar ratio. Re values for the UL-B0–UL-B5 films were slightly lower than those for the corresponding films PU, suggesting the introduction of NL, which increased the interaction between hard-segments caused by graft-reaction and multi-branched structure.

3.3. Graft-IPNs structure

As seen in Fig. 5, the introduction of NL simultaneously enhanced the strength and toughness of the materials. On the contrary, a material from PU and nitrokonjac glucomannan (NKGM) exhibited higher σ_b and lower ε_b than PU, owing

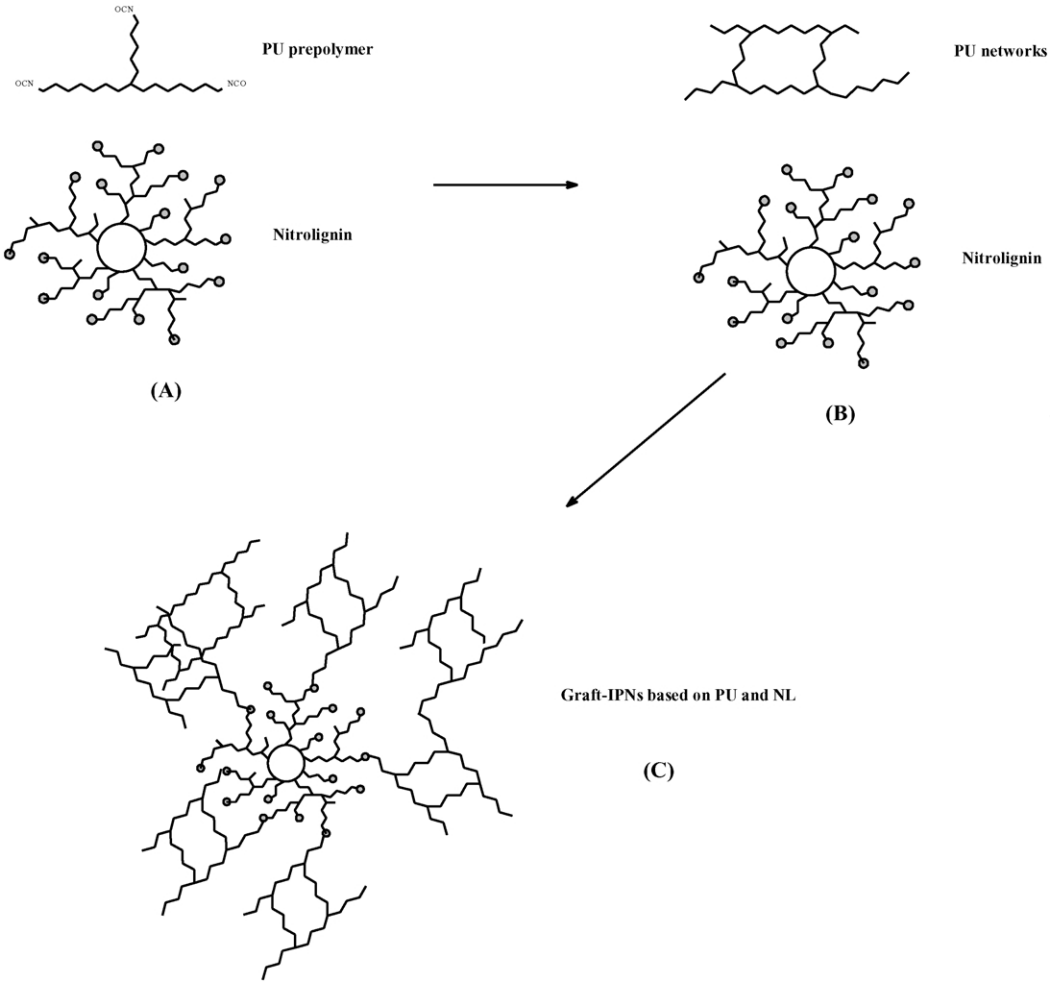

Fig. 8. Schematic structure of linear PU prepolymer and NL (A), PU networks and NL (B), and graft-IPNs based on PU and NL (C).

to the NKGM molecules, with $M_w = 14 \times 10^4$, penetrating into the PU networks under similar conditions to form semi-IPNs [26]. It must be mentioned that NL exhibited higher stiffness than NKGM, and the content was only 2.8 wt%. What happened after the addition of NL? In our previous work, it has been reported that NL in THF solution displays a dense random conformation, similar to an Einstein sphere, in consequence of a highly branched and networked structure with multi-active –OH [21]. It proved that –OH in NL exhibited higher reactive ability with –NCO of PU than that in nitrocellulose, and higher NL content decreased the mechanical properties [21]. Thus, a great star network by grafting with multi-PU network on an active NL molecule as the center was considered as the most possible structure, resulting in simultaneous enhancement of σ_b and ε_b. Therefore, the formation of graft-IPNs structure based on NL and PU networks can be depicted in Fig. 8. The PU prepolymer and NL exist in the mixture (Fig. 8(A)), and PU networks previously formed (Fig. 8(B)), and then PU networks were grafted on the NL. In this case, the NL molecule can react with multi-PU network and even with PU entangled network (Fig. 8(C)). The interpenetration and entanglement of such networks like a star not only simultaneously enhanced the strength and stiffness of materials, but also kept the retractability.

To understand active –OH of NL to react with PU to form graft-IPNs with higher cross-link density, the structure of the films with and without NL were compared by using solid-state CP/MAS ^{13} C NMR. ^{13}C NMR spectra of UL-B3 and PU-B3 are shown in Fig. 9. The contribution of NL on the spectra was neglected because of the low content of NL. Compared with PU-B3, the chemical shifts of C adjacent to urethane and in aromatic UL-B3 shifted to high chemical shift, indicating that the motion of PU chain was restricted. Simultaneously, such restriction of molecules was verified by electron spin resonance (ESR) in graft-IPNs based on PU and chitosan [18].

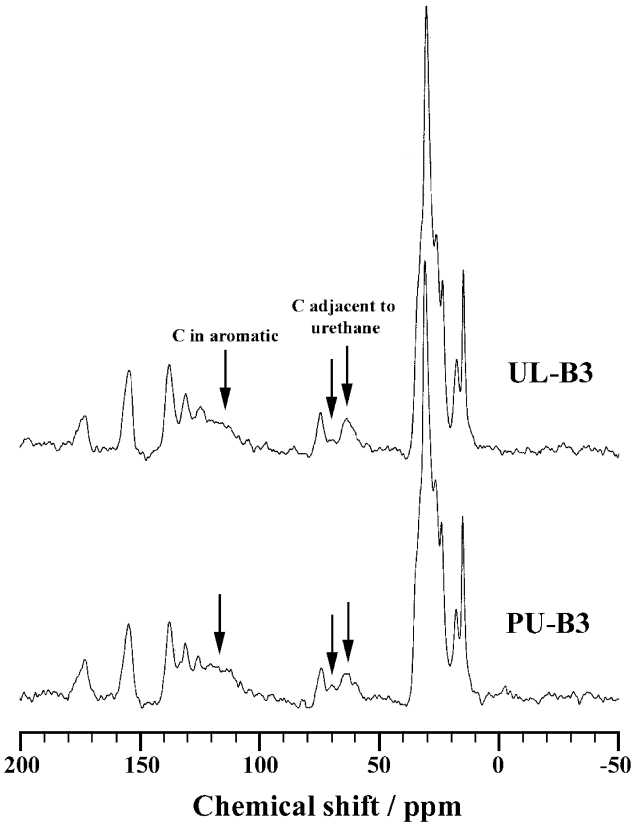

Fig. 9. Solid-state CP/MAS ^{13}C NMR spectra of UL-B3 and PU-B3.

4. Conclusion

A series of graft-IPNs were synthesized from castor oil-based PU with NCO/OH molar ratio 0.73–2.0 and 2.8 wt% NL (UL). All the UL films were nearly amorphous. With an increase of NCO/OH molar ratio, the glass transition temperature, the stiffness and tensile strength of the UL films increased, while breaking elongation and strain recoverability decreased. The UL films with 1.20 of NCO/OH molar ratio exhibited the maximum value of tensile strength. A little of NL plays an important role in the simultaneous enhancement of tensile strength and breaking elongation of the UL films due to its graft-reaction with PU network. Especially σ_b and ε_b of UL-B3 with NCO/OH molar ratio 1.20 were triple and 1.5 times, respectively than those of PU-B3. NMR showed that the introduction of NL into PU restricted the motion of PU molecules, indicating the relatively higher cross-link network structure in the UL films. Therefore, multi-PU networks were grafted on an active NL molecule as center to form relatively great network structures like star, namely graft-IPNs. Such graft-IPNs structure not only improved the strength and toughness of materials, but also kept the retractability.

Acknowledgements

This work was supported by the National Natural Science Foundation of China (59773026 and 59933070), Laboratory of Molecular Engineering in Polymers of Fudan University and Laboratory of Cellulose and Lignocellulosic Chemistry, Guangzhou Institute of Chemistry, Chinese Academic of Sciences.

References

[1] Petrovic ZS, Ferglson J. Prog Polym Sci 1991;16:695.
[2] Desai S, Thakore IM, Sarawae BD, Devi S. Eur Polym J 2000;36:711.
[3] Li Y, Kang W, Stoffer JO, Chu B. Macromolecules 1994;27:612.
[4] Song YM, Chen WC, Yu TL, Linliu K, Tseng YH. J Appl Polym Sci 1996;62:827.
[5] Pandya MV, Deshpande DD, Hundiwale DG. J Appl Polym Sci 1986;32:4959.
[6] Debowski M, Balas A. J Appl Polym Sci 2000;75:728.

[7] Yu TL, Lin TL, Tsai YM, Liu WJ. J Polym Sci, Polym Phys Ed 1999;37:2673.
[8] Hsu TF, Lee YD. Polymer 1999;40:577.
[9] Bae JY, Chung DJ, An JH, Shin DH. J Mater Sci 1999;34:2523.
[10] Harris RF, Joseph MD, Davison C, Deporter CD, Dais VA. J Appl Polym Sci 1990;41:509.
[11] Spathis G, Niaounakis M, Kontou E, Apekis L, Pissis P, Christodoulides C. J Appl Polym Sci 1994;54:831.
[12] Kontou E, Spathis G, Niaounakis M, Kefalas V. Colloid Polym Sci 1990;268:636.
[13] Hsu JM, Yang DL, Huang SK. Thermochim Acta 1999;333:73.
[14] Huang S, Lai J. Eur Polym J 1997;33:1563.
[15] Sperling LH. Interpenetrating polymer networks and related materials. New York: Plenum Press, 1981.
[16] Hsieh LH, Hung WY, Liao DC, Kao SC. J Appl Polym Sci 1995;57:319.
[17] Raymond MP, Bui VT. J Appl Polym Sci 1998;70:1649.
[18] Gong P, Zhang L, Zhuang L, Lu J. J Appl Polym Sci 1998;68:1321.
[19] Zhang L, Zhou J, Huang J, Gong P, Zhou Q. Ind Engng Chem Res 1999;38:4684.
[20] Wang J, Manley RSJ, Feldman D. Prog Polym Sci 1992;17:611.
[21] Zhang L, Huang J. J Appl Polym Sci 2001;80:1213.
[22] Zhang L, Huang J. J Appl Polym Sci 2001;81:3251.
[23] Hourston DJ, Zia Y. J Appl Polym Sci 1984;29:629.
[24] Darren JM, Gordon FM, Gordon MR, Pathiraja AG, Simon JM. J Appl Polym Sci 1996;60:557.
[25] Velankar S, Cooper SL. Macromolecules 1998;31:9181.
[26] Gao S, Zhang L. Macromolecules 2001;34:2202.